Reflection and refraction of multipole radiation by an interface

Henk F. Arnoldus

Department of Physics and Astronomy, Mississippi State University, P.O. Drawer 5167, Mississippi State, Mississippi, 39762-5167

Received May 1, 2004; revised manuscript received July 22, 2004; accepted July 22, 2004

Reflection and refraction of electromagnetic multipole radiation by an interface is studied. The multipole can be electric or magnetic and is of arbitrary order (dipole, quadrupole). From the angular spectrum representation of the radiation emitted by the multipole, I have obtained the angular spectrum representations of the reflected and transmitted fields, which involve the Fresnel reflection and transmission coefficients. The intensity distribution in the far field is evaluated with the method of stationary phase. The result is very simple in appearance and can be expressed in terms of two auxiliary functions of a complex variable. By exchanging the Fresnel coefficients for s and p polarization, the result for an electric multipole can be obtained from the result for a magnetic multipole.

OCIS codes: 240.0240, 260.2110.

1. INTRODUCTION

When a radiating atom is located near an interface, part of the emitted field serves as the incident field, giving rise to reflection and refraction. The reflected radiation, in turn, interacts with the atom and modifies the time evolution of the atomic density operator, leading to an enhanced or inhibited emission rate (or lifetime) as compared with the emission rate without the presence of the boundary. The influence of the interface on emission rates has been studied extensively, both experimentally[1–8] and theoretically,[9–11] and in particular the dependence on the separation distance between the atom and the surface of the medium. Also, the radiation pattern (angular intensity distribution) is affected by the reflection and transmission at the interface.[12,13] Of particular interest is the transmitted light for the case when the index of refraction of the substrate is larger than the index of refraction of the embedding medium of the source. Since the traveling waves emanating from the source bend toward the normal upon refraction, there exists a transmission angle $\theta_{\rm ac}$ such that in the angular region $\theta_{\rm ac} < \theta_t < \pi/2$, where θ_t is the transmission angle, there can be no radiation originating in traveling waves from the source. Any radiation observed in this region comes from evanescent waves that are converted into traveling waves at the interface and then end up in the far field. Observation of this light, which is sometimes called forbidden light,[14] opens the possibility of probing the source on a subwavelength scale.[15–22] The angle $\theta_{\rm ac}$ is called the anticritical angle[23] since it is the transmission angle at which the corresponding incident wave becomes evanescent, whereas the usual critical angle is the angle of incidence at which the transmitted waves becomes evanescent.

Most radiation emitted by atoms and molecules is electric dipole radiation, and the radiation from a localized source is in first approximation electric dipole radiation. However, when an atomic transition is dipole forbidden, higher-order multipole radiation can be emitted. In this paper I consider a source of radiation that emits a pure multipole field, either electric or magnetic, and of arbitrary order (dipole, quadrupole). The source is located in a medium with dielectric constant ε_1, a distance H above the xy plane, and located on the z axis. The region $-L < z < 0$ is a layer of material with dielectric constant ε_2, and the substrate $z < -L$ has dielectric constant ε_3. We shall assume that ε_1 is positive, but we do not impose any restrictions on the values of ε_2 and ε_3. For example, a negative value for the real part of ε_3 models a metal substrate. The corresponding indices of refraction are defined as $n_i = \sqrt{\varepsilon_i}$, $i = 1, 2, 3$. Figure 1 illustrates the situation.

2. MULTIPOLE FIELDS

We assume time-harmonic fields, oscillating with angular frequency ω, so that the electric field is represented as $\mathbf{E}(\mathbf{r}, t) = \mathrm{Re}[\mathbf{E}(\mathbf{r})\exp(-i\omega t)]$ with $\mathbf{E}(\mathbf{r})$ the complex amplitude, and similarly for the magnetic field $\mathbf{B}(\mathbf{r}, t)$. The electric field of a pure (α, l, m) multipole, located at the origin of coordinates, is proportional to the standard multipole vector potential $\mathbf{A}_{lm}(\mathbf{r}; \alpha)$ according to[24–26]

$$\mathbf{E}(\mathbf{r}) = \frac{ik_0{}^3}{4\pi\varepsilon_0} b_{lm}(\alpha)\mathbf{A}_{lm}(\mathbf{r}; \alpha), \tag{1}$$

with $k_0 = \omega/c$. The type of multipole is indicated by $\alpha = e$ for electric and $\alpha = m$ for magnetic. The possible values of l are $l = 1$ (dipole), $l = 2$ (quadrupole),..., and for each l the possible values of m are $m = -l, -l + 1, \ldots, l$. The constants $b_{lm}(\alpha)$ are the multipole coefficients, which are determined by the source (dipole moment, etc.), and they can be expressed in terms of the current density of the source.[27] The multipole vector potential for $\alpha = m$ is given by

$$\mathbf{A}_{lm}(\mathbf{r}; m) = h_l^{(1)}(n_1 k_0 r)\mathbf{T}_{llm}(\theta, \phi) \tag{2}$$

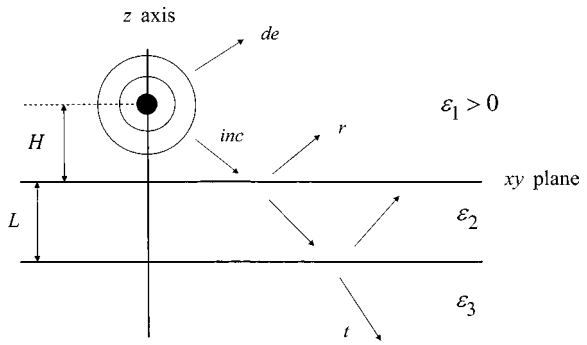

Fig. 1. Illustration of the multipole located on the z axis, a distance H above the xy plane, and embedded in a medium with dielectric constant ε_1. The layer has a thickness L and a dielectric constant ε_2. The substrate occupies the region $z < -L$ and is made of a material with dielectric constant ε_3. The circles around the multipole schematically indicate that the emitted radiation is a spherical wave. The arrows represent the wave vectors of the traveling partial waves of the angular spectrum, and the labels de, inc., r, and t indicate the directly emitted, incident, reflected, and transmitted waves, respectively.

in spherical coordinates (r, θ, ϕ). Here, $h_l^{(1)}(n_1 k_0 r)$ is a spherical Hankel function, and $\mathbf{T}_{llm}(\theta, \phi)$ is a vector spherical harmonic, defined in general as

$$\mathbf{T}_{jlm}(\theta, \phi) = \sum_{\mu' \mu} (l\mu' 1\mu | jm) Y_{l\mu'}(\theta, \phi) \mathbf{e}_\mu \tag{3}$$

in terms of Clebsch–Gordan coefficients $(l\mu' 1\mu | jm)$, spherical harmonics $Y_{l\mu'}(\theta, \phi)$, and spherical unit vectors $\mathbf{e}_\mu$. The multipole vector potential for $\alpha = e$ follows from $\mathbf{A}_{lm}(\mathbf{r}; m)$ as

$$\mathbf{A}_{lm}(\mathbf{r}; e) = -\frac{i}{n_1 k_0} \nabla \times \mathbf{A}_{lm}(\mathbf{r}; m). \tag{4}$$

The magnetic field of a multipole is determined by a Maxwell equation according to

$$\mathbf{B}(\mathbf{r}) = -\frac{i}{\omega} \nabla \times \mathbf{E}(\mathbf{r}). \tag{5}$$

3. ANGULAR SPECTRUM REPRESENTATION

The multipole fields from Section 2 are spherical waves emanating from the multipole in $\mathbf{r} = 0$. Such a representation is not suitable for the study of reflection and refraction of this radiation by an interface. More appropriate is the so-called angular spectrum representation, which is a superposition of plane waves, each of which satisfies Maxwell's equations in a medium with index of refraction n_1, but without any sources. An angular spectrum representation of the multipole vector potentials can be obtained[28,29] with a theorem due to Erdélyi,[30] derived for the scalar multipole fields. The result for $\mathbf{A}_{lm}(\mathbf{r}; m)$ is

$$\mathbf{A}_{lm}(\mathbf{r}, m) = \frac{(-i)^l}{2\pi n_1 k_0} \int \mathrm{d}^2 \mathbf{k}_\parallel \frac{1}{\beta} \times \exp(i\mathbf{K}_\pm \cdot \mathbf{r}) \mathbf{V}_{lm}(\pm\cos\bar{\theta}, \bar{\phi}). \tag{6}$$

The integration variable $\mathbf{k}_\parallel$ is a vector in the xy plane. Given $\mathbf{k}_\parallel$, the parameter β is defined as

$$\beta = \begin{cases} (n_1^2 k_0^2 - k_\parallel^2)^{1/2}, & k_\parallel < n_1 k_0 \\ i(k_\parallel^2 - n_1^2 k_0^2)^{1/2}, & k_\parallel > n_1 k_0 \end{cases}. \tag{7}$$

The wave vectors $\mathbf{K}_\pm$ are

$$\mathbf{K}_\pm = \mathbf{k}_\parallel \pm \beta \mathbf{e}_z, \tag{8}$$

and the upper (lower) sign is to be taken for the field in the region $z > 0$ $(z < 0)$. The factors $\exp(i\mathbf{K}_\pm \cdot \mathbf{r})$ in the integrand represent plane waves. From Eq. (7) we can see that $k_\parallel^2 + \beta^2 = n_1^2 k_0^2$, and therefore these partial waves of the angular spectrum satisfy the dispersion relation for a medium with dielectric constant n_1. For $k_\parallel < n_1 k_0$, parameter β is positive, and the wave travels in the direction of $\mathbf{K}_\pm$. Because of the $\pm$ in Eq. (8), the z component of $\mathbf{K}_\pm$ is positive and negative with z, and therefore the wave travels in a direction away from the xy plane on both sides, such that the parallel component $\mathbf{k}_\parallel$ is the same for $z > 0$ and $z < 0$. For $k_\parallel > n_1 k_0$, parameter β is positive imaginary, and the wave vector has an imaginary z component. This corresponds to a plane wave decaying away from the xy plane on both sides (evanescent wave) while still traveling in the $\mathbf{k}_\parallel$ direction along the xy plane.

We now define $\cos\bar{\theta}$ as

$$\cos\bar{\theta} = \frac{\beta}{n_1 k_0}, \tag{9}$$

and from Eq. (7) we can see that this quantity is either positive or positive imaginary. For $k_\parallel < n_1 k_0$, corresponding to a traveling wave, the angle $\bar{\theta}$ (taken as $0 \leqslant \bar{\theta} \leqslant \pi/2$) is the angle between the wave vector $\mathbf{K}_\pm$ and the z axis. This is the polar angle, measured from the positive z axis, of $\mathbf{K}_+$ and $\mathbf{K}_-$ and makes an angle of $\bar{\theta}$ with the negative z axis. When $k_\parallel > n_1 k_0$, corresponding to an evanescent wave, $\cos\bar{\theta}$ is imaginary and there is no angle $\bar{\theta}$ associated with this quantity. We then define $\sin\bar{\theta} = (1 - \cos^2\bar{\theta})^{1/2}$, which is larger than unity for an evanescent wave. The magnitude of $\mathbf{k}_\parallel$ can then be written as

$$k_\parallel = n_1 k_0 \sin\bar{\theta}, \tag{10}$$

and we indicate the polar angle of $\mathbf{k}_\parallel$ in the xy plane by $\bar{\phi}$. The wave vector then becomes

$$\mathbf{K}_\pm = n_1 k_0 \sin\bar{\theta}(\mathbf{e}_x \cos\bar{\phi} + \mathbf{e}_y \sin\bar{\phi}) + n_1 k_0 \mathbf{e}_z \cos\bar{\theta}. \tag{11}$$

The function $\mathbf{V}_{lm}(\pm\cos\bar{\theta}, \bar{\phi})$ in the integrand on the right-hand side of Eq. (6) is a generalized vector spherical harmonic, defined in Ref. 29. It is essentially the same function as $\mathbf{T}_{llm}(\theta, \phi)$, when expressed as a function of $\cos\theta$, but it allows for possible complex values of the first argument. The essential difference is that in Eq. (2) for the vector potential the function $\mathbf{T}_{llm}(\theta, \phi)$ depends on the spherical-coordinate angles (θ, ϕ) of the field point $\mathbf{r}$, whereas in $\mathbf{V}_{lm}(\pm\cos\bar{\theta}, \bar{\phi})$ the variables are functions of $\mathbf{k}_\parallel$, and there is no relation to the coordinates of the field point $\mathbf{r}$.

The angular spectrum representation of $\mathbf{A}_{lm}(\mathbf{r};\, e)$ follows from Eqs. (4) and (6), and we obtain

$$\mathbf{A}_{lm}(\mathbf{r},\, e) = \frac{(-i)^l}{2\pi n_1 k_0}\int \mathrm{d}^2\mathbf{k}_\parallel \frac{1}{\beta} \times \exp(i\mathbf{K}_\pm\cdot\mathbf{r})\hat{\mathbf{K}}_\pm \times \mathbf{V}_{lm}(\pm\cos\bar{\theta},\, \bar{\phi}), \tag{12}$$

with $\hat{\mathbf{K}}_\pm = \mathbf{K}_\pm/(n_1 k_0)$.

4. MULTIPOLE NEAR AN INTERFACE

The multipole fields from Section 2 are the fields radiated by a multipole at the origin of coordinates. An advantage of the angular spectrum representation, as given in Section 3, is that it allows us to shift the location of the multipole in a simple way since the dependence on the field point $\mathbf{r}$ enters only as $\exp(i\mathbf{K}_\pm\cdot\mathbf{r})$. As illustrated in Fig. 1, we consider a multipole located at $H\mathbf{e}_z$. Therefore in the angular spectrum representation of the fields we have only to replace $\exp(i\mathbf{K}_\pm\cdot\mathbf{r})$ by $\exp[i\mathbf{K}_\pm\cdot(\mathbf{r}-H\mathbf{e}_z)]$. We then have $i\mathbf{K}_\pm\cdot(-H\mathbf{e}_z) = \mp in_1 h\cos\bar{\theta}$, with $h = k_0 H$ the dimensionless distance between the multipole and the interface. From Eqs. (1) and (6) we then find for the electric field of a magnetic multipole at $H\mathbf{e}_z$

$$\mathbf{E}_s(\mathbf{r}) = -\frac{(-i)^{l+1}{k_0}^2}{8\pi^2\varepsilon_0 n_1} b_{lm}(m)\int \mathrm{d}^2\mathbf{k}_\parallel \frac{1}{\beta}\exp(i\mathbf{K}_\pm\cdot\mathbf{r} \mp in_1 h\cos\bar{\theta})\mathbf{V}_{lm}(\pm\cos\bar{\theta},\, \bar{\phi}), \tag{13}$$

where the subscript s indicates that this is the source field. Similarly, the source field for an electric multipole is

$$\mathbf{E}_s(\mathbf{r}) = -\frac{(-i)^{l+1}{k_0}^2}{8\pi^2\varepsilon_0 n_1} b_{lm}(e) \times \int \mathrm{d}^2\mathbf{k}_\parallel \frac{1}{\beta}\exp(i\mathbf{K}_\pm\cdot\mathbf{r} \mp in_1 h\cos\bar{\theta})\hat{\mathbf{K}}_\pm \times \mathbf{V}_{lm}(\pm\cos\bar{\theta},\, \bar{\phi}). \tag{14}$$

The upper and lowers signs now pertain to the fields in $z > H$ and $z < H$, respectively.

The fields with the upper signs will be referred to as the directly emitted (de) waves, and the fields with the lower signs as the incident (inc) fields. In the region $0 < z < H$, the source field serves as the incident field on the interface, and this gives rise to reflection and refraction. In $z > H$ the electric field can be written as

$$\mathbf{E}(\mathbf{r}) = \mathbf{E}_{\mathrm{de}}(\mathbf{r}) + \mathbf{E}_r(\mathbf{r}), \tag{15}$$

where r indicates the reflected field. Inside the layer the field has two contributions, as shown schematically in Fig. 1, due to multiple reflections at both boundaries. For $z < -L$, there is only the transmitted (t) field.

5. POLARIZED WAVES

Since each partial wave of the angular spectrum is a solution of Maxwell's equations for a source-free region with index of refraction n_1, we need only to consider the reflection and transmission of these plane waves. To use the standard results in terms of Fresnel coefficients, we have to decompose the partial waves in s- and p-polarized waves.[31–33] For a given $\mathbf{k}_\parallel$, we define the s polarization vector as

$$\mathbf{e}_{s\pm} = \hat{\mathbf{k}}_\parallel \times \mathbf{e}_z, \tag{16}$$

with $\hat{\mathbf{k}}_\parallel = \mathbf{k}_\parallel/k_\parallel$, and the subscript $\pm$ is added for later convenience. The p polarization vectors, related to the wave vectors $\hat{\mathbf{K}}_\pm$, are defined as

$$\mathbf{e}_{p\pm} = \hat{\mathbf{K}}_\pm \times \mathbf{e}_s, \tag{17}$$

and these can be expressed as

$$\mathbf{e}_{p\pm} = \pm\cos\bar{\theta}\hat{\mathbf{k}}_\parallel - \sin\bar{\theta}\mathbf{e}_z. \tag{18}$$

For evanescent waves, the polarization vectors $\mathbf{e}_{p\pm}$ are complex. The polarization vectors are normalized as $\mathbf{e}_{\sigma\pm}\cdot\mathbf{e}_{\sigma\pm} = 1$, $\sigma = s$, p, and we have $\hat{\mathbf{K}}_\pm\cdot\mathbf{e}_{\sigma\pm} = 0$. The generalized vector spherical harmonics have the property [Eq. (76) of Ref. 29]

$$\hat{\mathbf{K}}_\pm\cdot\mathbf{V}_{lm}(\pm\cos\bar{\theta},\, \bar{\phi}) = 0, \tag{19}$$

indicating that they have no $\hat{\mathbf{K}}_\pm$ component, and therefore we can write

$$\mathbf{V}_{lm}(\pm\cos\bar{\theta},\, \bar{\phi}) = \sum_\sigma \mathbf{e}_{\sigma\pm}[\mathbf{e}_{\sigma\pm}\cdot\mathbf{V}_{lm}(\pm\cos\bar{\theta},\, \bar{\phi})]. \tag{20}$$

Substitution into Eq. (13) yields the angular spectrum for the electric field of a magnetic multipole as a superposition of polarized plane waves of the form $\mathbf{e}_{\sigma\pm}\exp(i\mathbf{K}_\pm\cdot\mathbf{r})$. For the electric multipole we need to take the cross product of Eq. (20) with $\hat{\mathbf{K}}_\pm$, which yields terms with $\hat{\mathbf{K}}_\pm\times\mathbf{e}_{\sigma\pm}$ as polarization vectors. It can be shown by inspection that the cross product can be moved inside the square brackets in Eq. (20) as

$$\hat{\mathbf{K}}_\pm \times \mathbf{V}_{lm}(\pm\cos\bar{\theta},\, \bar{\phi}) = \sum_\sigma \mathbf{e}_{\sigma\pm}[(\mathbf{e}_{\sigma\pm}\times\hat{\mathbf{K}}_\pm)\cdot\mathbf{V}_{lm}(\pm\cos\bar{\theta},\, \bar{\phi})], \tag{21}$$

so that Eq. (14) also becomes a superposition of polarized waves of the form $\mathbf{e}_{\sigma\pm}\exp(i\mathbf{K}_\pm\cdot\mathbf{r})$. Comparison of Eqs. (20) and (21) then shows that the electric field of an electric multipole follows from the electric field of a magnetic multipole under the substitution $\mathbf{e}_{\sigma\pm}\to\mathbf{e}_{\sigma\pm}\times\hat{\mathbf{K}}_\pm$ for the polarization vector preceding the generalized vector spherical harmonic.

6. REFLECTION AND TRANSMISSION

Let us consider the field of the magnetic multipole first. The directly emitted field is given by Eq. (13) with the upper sign, and when we substitute expansion (20) with the upper sign we obtain explicitly

$$\mathbf{E}_{\mathrm{de}}(\mathbf{r}) = -\frac{(-i)^{l+1}k_0^2}{8\pi^2\varepsilon_0 n_1} b_{lm}(m) \int \mathrm{d}^2\mathbf{k}_\parallel \frac{1}{\beta} \times \exp(i\mathbf{K}_+ \cdot \mathbf{r} - in_1 h \cos\bar{\theta}) \times \sum_\sigma \mathbf{e}_{\sigma+}[\mathbf{e}_{\sigma+} \cdot \mathbf{V}_{lm}(\cos\bar{\theta}, \bar{\phi})]. \quad (22)$$

The incident field is given by the same expression, but with the lower signs, and therefore each incident wave is proportional to $\mathbf{e}_{\sigma-}\exp(i\mathbf{K}_- \cdot \mathbf{r})$. The corresponding reflected wave has wave vector $\mathbf{K}_+$ and polarization vector $\mathbf{e}_{\sigma+}$ and is multiplied by the Fresnel reflection coefficient $R_\sigma(\alpha)$. These Fresnel coefficients depend only on the wave vector through the dimensionless variable

$$\alpha = k_\parallel/k_0 = n_1 \sin\bar{\theta}. \quad (23)$$

The reflected field then becomes

$$\mathbf{E}_r(\mathbf{r}) = -\frac{(-i)^{l+1}k_0^2}{8\pi^2\varepsilon_0 n_1} b_{lm}(m) \int \mathrm{d}^2\mathbf{k}_\parallel \frac{1}{\beta} \times \exp(i\mathbf{K}_+ \cdot \mathbf{r} + in_1 h \cos\bar{\theta}) \times \sum_\sigma R_\sigma(\alpha)\mathbf{e}_{\sigma+}[\mathbf{e}_{\sigma-} \cdot \mathbf{V}_{lm}(-\cos\bar{\theta}, \bar{\phi})], \quad (24)$$

and the total field is $\mathbf{E}(\mathbf{r}) = \mathbf{E}_{\mathrm{de}}(\mathbf{r}) + \mathbf{E}_r(\mathbf{r})$.

The transmitted wave propagates in a medium with dielectric constant ε_3, and the wave vector $\mathbf{k}_t$, given $\mathbf{k}_\parallel$, is therefore

$$\mathbf{k}_t = \mathbf{k}_\parallel - k_0\nu_3\mathbf{e}_z, \quad (25)$$

in terms of the parameter

$$\nu_3 = (\varepsilon_3 - \alpha^2)^{1/2}. \quad (26)$$

Here it is understood that we take the principal value of the square root on the right-hand side (cut just below the negative real axis). The polarization vector for s polarization is again given by Eq. (16), and for p polarization we take

$$\mathbf{e}_{pt} = -\frac{1}{n_3}(\nu_3\hat{\mathbf{k}}_\parallel + \alpha\mathbf{e}_z). \quad (27)$$

The transmitted field then becomes

$$\mathbf{E}(\mathbf{r}) = -\frac{(-i)^{l+1}k_0^2}{8\pi^2\varepsilon_0 n_1} b_{lm}(m) \int \mathrm{d}^2\mathbf{k}_\parallel \frac{1}{\beta} \times \exp(i\mathbf{k}_t \cdot \mathbf{r} + in_1 h \cos\bar{\theta}) \times \sum_\sigma T_\sigma(\alpha)\mathbf{e}_{\sigma t}[\mathbf{e}_{\sigma-} \cdot \mathbf{V}_{lm}(-\cos\bar{\theta}, \bar{\phi})], \quad (28)$$

with $T_\sigma(\alpha)$ the Fresnel transmission coefficients.

The expressions for the various parts of the field of an electric multipole follow when we make the substitutions $\mathbf{e}_{\sigma\pm} \to \mathbf{e}_{\sigma\pm} \times \hat{\mathbf{K}}_\pm$ in the factors in side square brackets in Eqs. (22), (24), and (28) [and, of course, $b_{lm}(m) \to b_{lm}(e)$]. The explicit forms of the Fresnel reflection and transmission coefficients can be found in Appendix A of Ref. 13.

7. ASYMPTOTIC APPROXIMATION FOR $z > H$

In the previous sections we have derived angular spectrum representations for the electric fields emitted by magnetic and electric multipoles near the interface and the fields reflected and transmitted by the layer. The corresponding magnetic fields can be obtained from Eq. (5). Of particular interest are the fields in the radiation zone ($r \to \infty$), where they can be detected with a macroscopic device. We first consider the region $z > H$, where the field is the sum of the directly emitted and reflected field, and we first consider the magnetic multipole. An asymptotic approximation to an angular spectrum can be obtained with the method of stationary phase, in which it is asserted that the main contribution to the integrals over $\mathbf{k}_\parallel$ comes from the neighborhood of a stationary point in the $\mathbf{k}_\parallel$ plane.[34,35] Both the directly emitted and the reflected waves are waves with wave vectors $\mathbf{K}_+$. The stationary phase approximation for a given observation direction (θ, ϕ) then has the general form

$$\int \mathrm{d}^2\mathbf{k}_\parallel \frac{1}{\beta}\exp(i\mathbf{K}_+ \cdot \mathbf{r})g(\mathbf{k}_\parallel) \approx -\frac{2\pi i}{r}\exp(in_1k_0r)g(\mathbf{k}_{\parallel,1}) \quad (29)$$

for an arbitrary function $g(\mathbf{k}_\parallel)$. The stationary point is

$$\mathbf{k}_{\parallel,1} = n_1k_0 \sin\theta\mathbf{e}_\rho, \quad (30)$$

with $\mathbf{e}_\rho = \cos\phi\mathbf{e}_x + \sin\phi\mathbf{e}_y$ the radial unit vector in the xy plane.

Since $\mathbf{k}_\parallel = n_1k_0 \sin\bar{\theta}(\cos\bar{\phi}\mathbf{e}_x + \sin\bar{\phi}\mathbf{e}_y)$, we see immediately that in the stationary point $(\bar{\theta}, \bar{\phi})_1 = (\theta, \phi)$. From Eq. (23) we find that α in the stationary point is equal to $n_1 \sin\theta$, which we indicate by α_1, and with $\hat{\mathbf{k}}_{\parallel,1} = \mathbf{e}_\rho$ we find from Eq. (16) that $(\mathbf{e}_{s\pm})_1 = -\mathbf{e}_\phi$. For the p polarization vectors we set $(\bar{\theta})_1 = \theta$ and $\hat{\mathbf{k}}_{\parallel,1} = \mathbf{e}_\rho$ in Eq. (18), which gives $(\mathbf{e}_{p+})_1 = \mathbf{e}_\theta$ and

$$(\mathbf{e}_{p-})_1 = -\cos\theta\mathbf{e}_\rho - \sin\theta\mathbf{e}_z. \quad (31)$$

Combining everything then yields the asymptotic approximation for the directly emitted and reflected fields of the magnetic multipole:

$$\mathbf{E}_{\mathrm{de}}(\mathbf{r}) \approx \frac{(-i)^l k_0^2}{4\pi\varepsilon_0 n_1 r} b_{lm}(m)\exp[in_1(k_0r - h\cos\theta)] \times \{\mathbf{e}_\theta[\mathbf{e}_\theta \cdot \mathbf{V}_{lm}(\cos\theta, \phi)] + \mathbf{e}_\phi[\mathbf{e}_\phi \cdot \mathbf{V}_{lm}(\cos\theta, \phi)]\}, \quad (32)$$

$$\mathbf{E}_r(\mathbf{r}) \approx \frac{(-i)^l k_0^2}{4\pi\varepsilon_0 n_1 r} b_{lm}(m)\exp[in_1(k_0r + h\cos\theta)] \times \{-R_p(\alpha_1)\mathbf{e}_\theta[(\cos\theta\mathbf{e}_\rho + \sin\theta\mathbf{e}_z) \cdot \mathbf{V}_{lm}(-\cos\theta, \phi)] + R_s(\alpha_1)\mathbf{e}_\phi[\mathbf{e}_\phi \cdot \mathbf{V}_{lm}(-\cos\theta, \phi)]\}. \quad (33)$$

The directly emitted field has an overall factor of $\exp(-in_1h\cos\theta)$ whereas the reflected field has a factor of $\exp(in_1h\cos\theta)$. These different factors account for the difference in travel distance from the source to the field point: The directly emitted waves travel directly toward the detector, but the reflected waves first travel to the surface and then reflect.

It can be shown from Eqs. (61) and (62) of Ref. 29 that the generalized vector spherical harmonics have the properties

$$\mathbf{e}_\rho\cdot\mathbf{V}_{lm}(-\cos\theta,\ \phi)=(-1)^{l+m+1}\mathbf{e}_\rho\cdot\mathbf{V}_{lm}(\cos\theta,\ \phi), \tag{34}$$

$$\mathbf{e}_z\cdot\mathbf{V}_{lm}(-\cos\theta,\ \phi)=(-1)^{l+m}\mathbf{e}_z\cdot\mathbf{V}_{lm}(\cos\theta,\ \phi), \tag{35}$$

$$\mathbf{e}_\phi\cdot\mathbf{V}_{lm}(-\cos\theta,\ \phi)=(-1)^{l+m+1}\mathbf{e}_\phi\cdot\mathbf{V}_{lm}(\cos\theta,\ \phi). \tag{36}$$

With $\mathbf{e}_\theta=\cos\theta\mathbf{e}_\rho-\sin\theta\mathbf{e}_z$ we then have

$$\begin{aligned}(\cos\theta\mathbf{e}_\rho+\sin\theta\mathbf{e}_z)\ \cdot\ \mathbf{V}_{lm}(-\cos\theta,\ \phi)\\ =(-1)^{l+m+1}\mathbf{e}_\theta\cdot\mathbf{V}_{lm}(\cos\theta,\ \phi),\end{aligned} \tag{37}$$

which can be used to simplify approximation (33). Then we add approximations (32) and (33) to obtain the total field in $z>H$:

$$\begin{aligned}\mathbf{E}(\mathbf{r})\approx{}&\frac{(-i)^l{k_0}^2}{4\pi\varepsilon_0n_1r}b_{lm}(m)\exp[in_1(k_0r-h\cos\theta)]\\ &\times\{[1+(-1)^{l+m}R_p(\alpha_1)\exp(2in_1h\cos\theta)]\\ &\times\mathbf{e}_\theta[\mathbf{e}_\theta\cdot\mathbf{V}_{lm}(\cos\theta,\ \phi)]\\ &+[1-(-1)^{l+m}R_s(\alpha_1)\exp(2in_1h\cos\theta)]\\ &\times\mathbf{e}_\phi[\mathbf{e}_\phi\cdot\mathbf{V}_{lm}(\cos\theta,\ \phi)]\}.\end{aligned} \tag{38}$$

The asymptotic approximation for an electric multipole can be obtained in the same way. The result is effectively the following: Replace $b_{lm}(m)$ by $b_{lm}(e)$ in approximation (38), switch $R_s(\alpha_1)$ and $R_p(\alpha_1)$, and take $\hat{\mathbf{r}}\times\ldots$. We can obtain the magnetic field from Eq. (5) before making the asymptotic approximation. When we then make the asymptotic approximation, it appears that the magnetic field is given by

$$\mathbf{B}(\mathbf{r})\approx\frac{n_1}{c}\hat{\mathbf{r}}\times\mathbf{E}(\mathbf{r}) \tag{39}$$

for both magnetic and electric multipoles.

8. ASYMPTOTIC APPROXIMATION FOR $z<-L$

The region $z<-L$ is occupied with a material with dielectric constant ε_3. When ε_3 has an imaginary part or a negative real part (metal), then there is no far field in $z<-L$. Therefore, when considering the far field in $z<-L$, we assume $\varepsilon_3>0$. The wave vectors of the partial waves are $\mathbf{k}_t$, and the general form of the stationary phase approximation, given (θ,ϕ), is

$$\begin{aligned}\int\mathrm{d}^2\mathbf{k}_\parallel\frac{1}{\beta}\exp(i\mathbf{k}_t\cdot\mathbf{r})g(\mathbf{k}_\parallel)\approx{}&\frac{2\pi i}{r}\frac{n_3\cos\theta}{n_1(\cos\bar{\theta})_3}\\ &\times\exp(in_3k_0r)g(\mathbf{k}_{\parallel,3}).\end{aligned} \tag{40}$$

The stationary point for medium n_3 is given by

$$\mathbf{k}_{\parallel,3}=n_3k_0\sin\theta\mathbf{e}_\rho. \tag{41}$$

The extra factor appearing in approximation (40), as compared with approximation (29), comes from $1/\beta$ in the integrand, which refers to the z component of the wave vector in medium n_1 rather than n_3.

The direction of $\mathbf{k}_{\parallel,3}$ in the xy plane is ϕ, so $(\bar{\phi})_3=\phi$. With $k_{\parallel,3}=n_3k_0\sin\theta$ and Eq. (23), we can see that the value of α in the stationary point is $\alpha_3=n_3\sin\theta$, and this becomes the argument of the Fresnel transmission coefficients $T_\sigma(\alpha)$. Again with Eq. (23) we find $(\sin\bar{\theta})_3=\alpha_3/n_1=(n_3/n_1)\sin\theta$, and therefore $\bar{\theta}$ in the stationary point is not equal to θ. We introduce $\sin\hat{\theta}$ as

$$\sin\hat{\theta}=\frac{n_3}{n_1}\sin\theta, \tag{42}$$

which can be larger than unity for $n_3>n_1$. Then we set $\cos\hat{\theta}=-(1-\sin^2\hat{\theta})^{1/2}$, which is negative or negative imaginary and equals $-(\cos\bar{\theta})_3$. In Eq. (28) for the transmitted field we have four unit polarization vectors that have to be evaluated in the stationary point. For s polarization we find $(\mathbf{e}_{s^-})_3=(\mathbf{e}_{st})_3=-\mathbf{e}_\phi$. From Eq. (18) we find

$$(\mathbf{e}_{p^-})_3=\cos\hat{\theta}\mathbf{e}_\rho-\sin\hat{\theta}\mathbf{e}_z \tag{43}$$

since $\hat{\mathbf{k}}_{\parallel,3}=\mathbf{e}_\rho$. From Eq. (26) we have $(\nu_3)_3=n_3|\cos\theta|$; and since $\pi/2<\theta<\pi$ for $z<-L$, this is $(\nu_3)_3=-n_3\cos\theta$. With Eq. (27) we then find $(\mathbf{e}_{pt})_3=\mathbf{e}_\theta$. We furthermore introduce modified transmission coefficients by

$$\hat{T}_\sigma(\alpha)=\frac{\nu_3}{\nu_1}T_\sigma(\alpha), \tag{44}$$

with $\nu_1=(\varepsilon_1-\alpha^2)^{1/2}$, in analogy with Eq. (26). Combining everything then yields the asymptotic approximation for the transmitted field of a magnetic multipole:

$$\begin{aligned}\mathbf{E}(\mathbf{r})\approx{}&\frac{(-i)^l{k_0}^2}{4\pi\varepsilon_0n_1r}b_{lm}(m)\exp(in_3k_0r-in_1h\cos\hat{\theta})\\ &\times\{\hat{T}_p(\alpha_3)\mathbf{e}_\theta[(\cos\hat{\theta}\mathbf{e}_\rho-\sin\hat{\theta}\mathbf{e}_z)\\ &\cdot\ \mathbf{V}_{lm}(\cos\hat{\theta},\ \phi)]\\ &+\hat{T}_s(\alpha_3)\mathbf{e}_\phi[\mathbf{e}_\phi\cdot\mathbf{V}_{lm}(\cos\hat{\theta},\ \phi)]\}.\end{aligned} \tag{45}$$

The result for an electric multipole follows from our replacing $b_{lm}(m)$ by $b_{lm}(e)$, switching $\hat{T}_s(\alpha_3)$ and $\hat{T}_p(\alpha_3)$, and by taking $\hat{\mathbf{r}}\times\ldots$ of approximation (45). The magnetic field is

$$\mathbf{B}(\mathbf{r})\approx\frac{n_3}{c}\hat{\mathbf{r}}\times\mathbf{E}(\mathbf{r}) \tag{46}$$

for both magnetic and electric multipoles.

When we detect the field at the polar angle θ, the angle of transmission is $\theta_t = \pi - \theta$ (measured from the negative z axis), since $\theta > \pi/2$. For $\hat{\theta}$ (if real), the sine is positive and the cosine is defined as negative, so $\pi/2 < \hat{\theta} < \pi$. If we let $\theta_{\rm inc} = \pi - \hat{\theta}$, then Eq. (42) becomes $n_1 \sin\theta_{\rm inc} = n_3 \sin\theta_t$, which is Snell's law of refraction; therefore $\theta_{\rm inc}$ is the angle of incidence of a plane wave from the angular spectrum corresponding to the transmitted plane wave that is detected at angle θ. We furthermore see from Eq. (42) that, for $n_3 > n_1$, $\sin\hat{\theta}$ can become larger than unity. Borderline is $\sin\hat{\theta} = 1$, which corresponds to $\theta_{\rm inc} = \pi/2$, and this occurs at a transmission angle $\theta_{\rm ac}$ given by

$$\sin\theta_{\rm ac} = \frac{n_1}{n_3}. \tag{47}$$

In other words, for detection of a traveling wave at transmission angle θ_t, with $0 \leqslant \theta_t < \theta_{\rm ac}$ the corresponding incident wave is traveling and for θ_t in the range $\theta_{\rm ac} < \theta_t < \pi/2$ the incident wave is evanescent. So $\theta_{\rm ac}$ is the transmission angle at which the incident waves turn evanescent, as mentioned in Section 1.

9. INTENSITY DISTRIBUTION

Having obtained the electric and magnetic fields of a multipole in the radiation zone, we now consider the intensity distribution as a function of θ and ϕ. From here on we shall write an equal sign instead of an approximation sign. The Poynting vector for time-harmonic fields is defined as

$$\mathbf{S}(\mathbf{r}) = \frac{1}{2\mu_0}\mathrm{Re}\,\mathbf{E}(\mathbf{r}) \times \mathbf{B}(\mathbf{r})^*. \tag{48}$$

With approximation (39) or (46) we can express the magnetic field in terms of the electric field, and with $\hat{\mathbf{r}} \cdot \mathbf{E}(\mathbf{r}) = 0$ the expression for the Poynting vector simplifies to

$$\mathbf{S}(\mathbf{r}) = \frac{n}{2\mu_0 c}[\mathbf{E}(\mathbf{r}) \cdot \mathbf{E}(\mathbf{r})^*]\hat{\mathbf{r}}, \tag{49}$$

where $n = n_1$ for $z > H$ and $n = n_3$ for $z < -L$. The emitted power per unit solid angle is $\mathrm{d}P/\mathrm{d}\Omega = r^2\mathbf{S}(\mathbf{r}) \cdot \hat{\mathbf{r}}$, and this becomes

$$\frac{\mathrm{d}P}{\mathrm{d}\Omega} = \frac{n}{2\mu_0 c} r^2 \mathbf{E}(\mathbf{r}) \cdot \mathbf{E}(\mathbf{r})^*. \tag{50}$$

We normalize this as

$$\frac{\mathrm{d}P}{\mathrm{d}\Omega} = P_1 \mathcal{N}_{lm}(\hat{\mathbf{r}};\, \alpha), \tag{51}$$

with P_1 the power emitted by an $(\alpha,\, l,\, m)$ multipole in a medium with index of refraction n_1, but without any boundaries. This power is explicitly

$$P_1 = \frac{1}{2n_1\mu_0 c}\left(\frac{k_0^{\,2}}{4\pi\varepsilon_0}\right)^2 |b_{lm}(\alpha)|^2. \tag{52}$$

We shall use this normalization for both the regions $z > H$ and $z < -L$.

For $z > H$ we find from approximation (38)

$$\begin{aligned}\mathcal{N}_{lm}(\hat{\mathbf{r}};\, m) = {} & |1 + (-1)^{l+m} R_p(\alpha_1) \\ & \times \exp(2in_1 h\cos\theta)|^2 |\mathbf{e}_\theta \cdot \mathbf{V}_{lm}(\cos\theta,\, \phi)|^2 \\ & + |1 - (-1)^{l+m} R_s(\alpha_1) \\ & \times \exp(2in_1 h\cos\theta)|^2 |\mathbf{e}_\phi \cdot \mathbf{V}_{lm}(\cos\theta,\, \phi)|^2;\end{aligned} \tag{53}$$

and if $\varepsilon_3 > 0$, we have from approximation (45)

$$\begin{aligned}\mathcal{N}_{lm}(\hat{\mathbf{r}};\, m) = {} & \frac{n_3}{n_1}\exp(2n_1 h\,\mathrm{Im}\cos\hat{\theta})[|\hat{T}_p(\alpha_3)|^2 |(\cos\hat{\theta}\mathbf{e}_\rho \\ & - \sin\hat{\theta}\mathbf{e}_z) \cdot \mathbf{V}_{lm}(\cos\hat{\theta},\, \phi)|^2 \\ & + |\hat{T}_s(\alpha_3)|^2 |\mathbf{e}_\phi \cdot \mathbf{V}_{lm}(\cos\hat{\theta},\, \phi)|^2].\end{aligned} \tag{54}$$

For the electric multipole we have to replace $b_{lm}(m)$ by $b_{lm}(e)$, but this has no effect on the normalized intensity distribution $\mathcal{N}_{lm}(\hat{\mathbf{r}};\, \alpha)$ since this constant is absorbed in P_1. Then we have to replace $\mathbf{E}(\mathbf{r})$ by $\hat{\mathbf{r}} \times \mathbf{E}(\mathbf{r})$, but this also has no effect since $[\hat{\mathbf{r}} \times \mathbf{E}(\mathbf{r})] \cdot [\hat{\mathbf{r}} \times \mathbf{E}(\mathbf{r})^*] = \mathbf{E}(\mathbf{r}) \cdot \mathbf{E}(\mathbf{r})^*$. Therefore $\mathcal{N}_{lm}(\hat{\mathbf{r}};\, e)$ simply follows from Eqs. (53) and (54) by an exchange of the s and p Fresnel coefficients.

10. FURTHER SIMPLIFICATIONS OF THE INTENSITY DISTRIBUTION

It can be shown that the generalized vector spherical harmonics have the properties

$$\mathbf{e}_\rho \cdot \mathbf{V}_{lm}(z,\, \phi) = \exp(im\phi)\mathbf{e}_x \cdot \mathbf{V}_{lm}(z,\, 0), \tag{55}$$

$$\mathbf{e}_\phi \cdot \mathbf{V}_{lm}(z,\, \phi) = \exp(im\phi)\mathbf{e}_y \cdot \mathbf{V}_{lm}(z,\, 0), \tag{56}$$

$$\mathbf{e}_z \cdot \mathbf{V}_{lm}(z,\, \phi) = \exp(im\phi)\mathbf{e}_z \cdot \mathbf{V}_{lm}(z,\, 0), \tag{57}$$

for arbitrary complex z. We set $z = \cos\theta$ and $z = \cos\hat{\theta}$ in Eqs. (53) and (54), respectively. Since the phase factors $\exp(im\phi)$ appear inside absolute value signs, these cancel, and there is no ϕ dependence left in $\mathcal{N}_{lm}(\hat{\mathbf{r}};\, \alpha)$. Furthermore, it can be shown that

$$\mathbf{e}_x \cdot \mathbf{V}_{l,-m}(z,\, 0) = (-1)^{m+1}\mathbf{e}_x \cdot \mathbf{V}_{lm}(z,\, 0), \tag{58}$$

$$\mathbf{e}_\nu \cdot \mathbf{V}_{l,-m}(z,\, 0) = (-1)^{m}\mathbf{e}_x \cdot \mathbf{V}_{lm}(z,\, 0), \tag{59}$$

$$\mathbf{e}_z \cdot \mathbf{V}_{l,-m}(z,\, 0) = (-1)^{m+1}\mathbf{e}_z \cdot \mathbf{V}_{lm}(z,\, 0), \tag{60}$$

and therefore the intensity distribution is independent of the sign of m.

Another property that can be derived for the generalized vector spherical harmonics is

$$\begin{aligned}&[\cos\beta(\cos\phi\mathbf{e}_x + \sin\phi\mathbf{e}_y) - \sin\beta\mathbf{e}_z] \cdot \mathbf{V}_{lm}(\cos\beta,\, \phi) \\ &\quad = -\frac{1}{\sin\beta}\mathbf{e}_z \cdot \mathbf{V}_{lm}(\cos\beta,\, \phi),\end{aligned} \tag{61}$$

where $\cos\beta$ can be complex. After using Eqs. (55)–(57), we need this result only for $\phi = 0$. Then we introduce the auxiliary functions

$$f_{lm}(z) = \frac{1}{|1 - z^2|}|\mathbf{e}_z \cdot \mathbf{V}_{lm}(z, 0)|^2, \tag{62}$$

$$g_{lm}(z) = |\mathbf{e}_y \cdot \mathbf{V}_{lm}(z, 0)|^2, \tag{63}$$

for complex z. The final result for the intensity distribution then becomes

$$\begin{aligned}\mathcal{N}_{lm}(\hat{\mathbf{r}}; m) = {} & |1 + (-1)^{l+m}R_p(\alpha_1) \\ & \times \exp(2in_1h\cos\theta)|^2 f_{lm}(\cos\theta) \\ & + |1 - (-1)^{l+m}R_s(\alpha_1) \\ & \times \exp(2in_1h\cos\theta)|^2 g_{lm}(\cos\theta),\end{aligned} \tag{64}$$

$$\begin{aligned}\mathcal{N}_{lm}(\hat{\mathbf{r}}; m) = {} & \frac{n_3}{n_1}\exp(2n_1h\,\mathrm{Im}\cos\hat{\theta}) \\ & \times [|\hat{T}_p(\alpha_3)|^2 f_{lm}(\cos\hat{\theta}) \\ & + |\hat{T}_s(\alpha_3)|^2 g_{lm}(\cos\hat{\theta})]\end{aligned} \tag{65}$$

for $z > H$ and $z < -L$, respectively.

11. DISCUSSION OF THE RESULT

Let us first consider a multipole in medium n_1, but without any boundaries (free multipole). The Fresnel coefficients become $R_\sigma = 0$, $T_\sigma = 1$, and in the above result we set $n_3 = n_1$. With Eq. (44) we then also have $\hat{T}_\sigma = 1$, and from Eq. (42) and $\cos\hat{\theta} < 0$ we find that $\hat{\theta}$ is equal to θ. Then $\mathrm{Im}\cos\hat{\theta} = 0$ and the overall exponential in Eq. (65) disappear. We then have

$$\mathcal{N}_{lm}(\hat{\mathbf{r}}; \alpha) = f_{lm}(\cos\theta) + g_{lm}(\cos\theta) \tag{66}$$

for both $z > H$ and $z < -L$. Since there is no longer a dependence on H and L, this holds for all $\hat{\mathbf{r}}$; and since there are no Fresnel coefficients left, there is no longer any distinction between magnetic and electric multipoles. The distribution is also independent of the index of refraction of the embedding medium. Equation (66) can also be written as

$$\mathcal{N}_{lm}(\hat{\mathbf{r}}; \alpha) = \mathbf{V}_{lm}(\cos\theta, 0) \cdot \mathbf{V}_{lm}(\cos\theta, 0)^*. \tag{67}$$

From $\mathbf{V}_{lm}(\cos\theta, 0) = \mathbf{T}_{llm}(\cos\theta, 0)$ and the fact that the usual vector spherical harmonics are normalized for integration over the unit sphere, we have $\int \mathrm{d}\Omega\mathcal{N}_{lm}(\hat{\mathbf{r}}; \alpha) = 1$. This shows that the constant P_1 is indeed the power emitted by the multipole in medium n_1.

Because of the boundary, reflected waves appear in $z > H$, with amplitudes proportional to the Fresnel reflection coefficients $R_\sigma(\alpha_1)$. They are multiplied by the retardation factor $\exp(2in_1h\cos\theta)$, which accounts for the difference in travel distance between directly emitted and reflected waves. The result is interference between the directly emitted waves (the 1 inside the absolute value signs) and the reflected waves. The overall functions $f_{lm}(\cos\theta)$ and $g_{lm}(\cos\theta)$ account essentially for the angular distribution of a free multipole, but because the Fresnel reflection coefficients for s and p waves are different, Eq. (64) splits into two terms. It should be noted that the additional minus sign in front of $R_s(\alpha_1)$, as compared with $R_p(\alpha_1)$, is a result of our phase convention for the polarization vectors. It is interesting to note that the Fresnel coefficients are multiplied by $(-1)^{l+m}$, which represents a phase shift upon reflection. Apparently, this phase shift depends on the l and m values of the multipole and is the same for all angles θ.

The radiation in $z < -L$ contains only transmitted waves, so there is no interference. The amplitudes of the transmitted waves are multiplied by a Fresnel transmission coefficient and an additional factor [Eq. (44)]. It is interesting to see that Eq. (65) also splits into two terms because of the difference in s and p waves and that the overall factors of each term are the same functions f_{lm} and g_{lm} as for the reflected waves in Eq. (64). The difference is that the argument of these functions here is $\cos\hat{\theta}$, which refers to the angle of incidence rather than the angle of transmission (or observation). As explained in Section 8, for $\theta_t > \theta_{\mathrm{ac}}$ the angle of incidence exceeds $\pi/2$, and the incident wave is evanescent. This makes $\cos\hat{\theta}$ negative imaginary, and the overall factor $\exp(2n_1h\,\mathrm{Im}\cos\hat{\theta})$ decays rapidly with the dimensionless multipole surface distance h, which is a reflection of the fact that the evanescent waves emitted by the multipole at $z = H$ decay exponentially in the direction toward the surface.

12. DIPOLES AND QUADRUPOLES

For a magnetic or an electric dipole we have $l = 1$, and the four auxiliary functions that determine the intensity distribution are

$$f_{11}(z) = \frac{3}{16\pi}, \tag{68}$$

$$g_{11}(z) = \frac{3}{16\pi}|z|^2, \tag{69}$$

$$f_{10}(z) = 0, \tag{70}$$

$$g_{10}(z) = \frac{3}{8\pi}|1 - z^2|. \tag{71}$$

Figure 2 shows a typical radiation pattern for $n_1 > n_3$. In the region $z > H$ we observe a lobe structure, which is due to interference between the directly emitted waves and the reflected waves at the interface. The distribution for the magnetic and electric dipole are very similar and indistinguishable for $z < -L$ for the parameters used in Fig. 2. In Fig. 3, where $n_3 > n_1$ and $m = 1$, we can see that most of the intensity ends up in the region $z < -L$. The electric dipole has a lobe near the anticritical angle and a smooth distribution for $0 \leqslant \theta_t < \theta_{\mathrm{ac}}$. The intensity distribution of the magnetic dipole has a sharp spike at θ_{ac}. For $m = 0$ this behavior approximately reverses.

For quadrupole radiation, for which $l = 2$, the auxiliary functions are

$$f_{22}(z) = \frac{5}{16\pi}|1 - z^2|, \tag{72}$$

$$g_{22}(z) = \frac{5}{16\pi}|1 - z^2||z|^2, \tag{73}$$

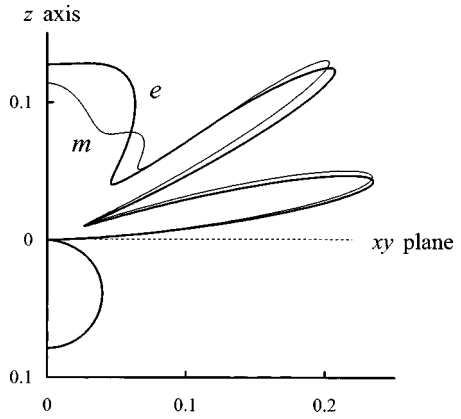

Fig. 2. Illustration of the intensity distribution $\mathcal{N}_{11}(\hat{\mathbf{r}};\ \alpha)$ for $\alpha = e$ and $\alpha = m$. The dimensionless distance between the dipole and the surface is $h = 1.8\pi$ (almost a wavelength) and $l = 0$ (single interface). The dielectric constants are $\varepsilon_1 = 1.5$ and $\varepsilon_3 = 1$.

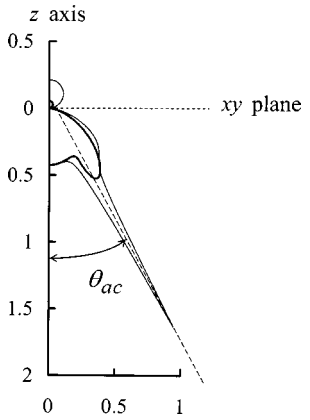

Fig. 3. Intensity distribution for dipole radiation with $m = 1$. The thin curve is for a magnetic dipole and the thick curve for an electric dipole. The parameters are $h = l = 0$, $\varepsilon_1 = 1$, and $\varepsilon_3 = 4$. The anticritical angle is 30°.

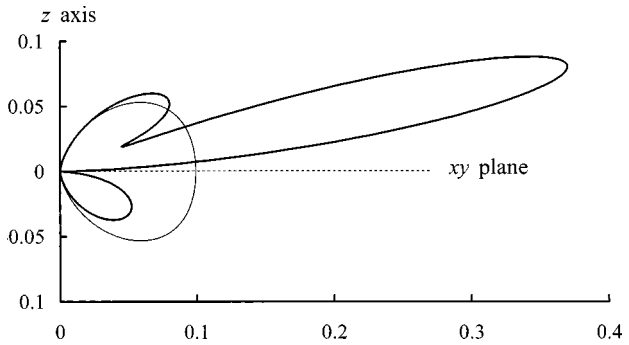

Fig. 4. Intensity distribution of electric quadrupole radiation with $m = 2$ for a free quadrupole (thin curve) and for a quadrupole near an interface (thick curve). For the free quadrupole the intensity distribution is independent of the dielectric constant ε_1 and the height h. For the quadrupole near the interface the parameters are $h = \pi$, $l = 0$, $\varepsilon_1 = 2$, and $\varepsilon_3 = 1.7$.

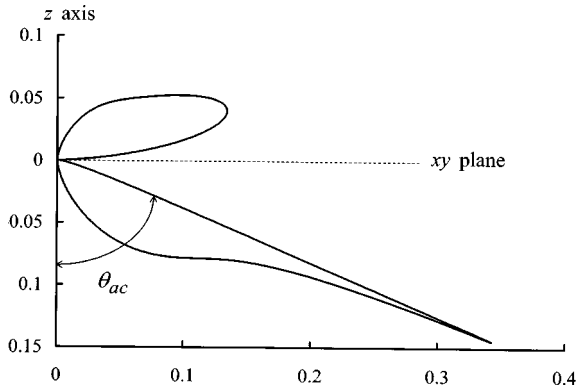

Fig. 5. Radiation pattern for an electric quadrupole with $m = 2$ near an interface. We took $h = \pi$ and $l = 0$, and the dielectric constants are $\varepsilon_1 = 1.7$ and $\varepsilon_3 = 2$ so that $\theta_{ac} = 67°$.

$$f_{21}(z) = \frac{5}{16\pi}|z|^2, \tag{74}$$

$$g_{21}(z) = \frac{5}{16\pi}|2z^2 - 1|^2, \tag{75}$$

$$f_{20}(z) = 0, \tag{76}$$

$$g_{20}(z) = \frac{15}{8\pi}|1 - z^2||z|^2. \tag{77}$$

Figure 4 shows the intensity distribution for an electric quadrupole with $m = 2$ near the interface and the corresponding distribution for the same free quadrupole. Since $n_1 > n_3$, most radiation is emitted in the direction $z > H$, and we can see the appearance of a very strong peak due to interference. For Fig. 5, the indices of refraction are exchanged, as compared with Fig. 4, but all other parameters are the same. The dimensionless height is $h = \pi$, corresponding to half a wavelength. The distribution has a sharp cutoff at θ_{ac}, which is due to the fact that the radiation in the range $\theta_{ac} < \theta_t < \pi/2$ has it origin in evanescent waves from the quadrupole. Already for the modest value of $h = \pi$ it appears that the evanescent waves do not reach the surface with sufficient amplitude to contribute to the refracted far field.

13. CONCLUSIONS

From the angular spectrum representation for the radiation emitted by a magnetic and an electric multipole of arbitrary order, an angular spectrum representation for the reflected and refracted fields by an interface has been derived. The reflected and transmitted fields were expressed in terms of Fresnel reflection and transmission coefficients, and this includes the situation shown in Fig. 1 where the interface consists of a layer and a substrate. With the method of stationary phase, an asymptotic approximation for the far field, both in $z > H$ and $z < -L$, was derived. The resulting intensity distribution could be expressed in terms of two universal auxiliary functions $f_{lm}(z)$ and $g_{lm}(z)$, defined in terms of generalized vector spherical harmonics. For radiation emitted

in the $z > H$ direction, we have $z = \cos\theta$ with θ the observation direction. For $z < -L$ this variable is $z = \cos\hat{\theta}$, which equals $\cos\hat{\theta} = -[1 - (\varepsilon_3/\varepsilon_1)\sin^2\theta]^{1/2}$. With Snell's law we then see that $\cos\hat{\theta} = -\cos\theta_{\text{inc}}$ for the case in which the incident wave is traveling, given the observation direction θ. On the other hand, for an evanescent incident wave, $\cos\hat{\theta}$ is imaginary. This corresponds to the situation in which an evanescent wave is converted into a traveling wave by the interface, and subsequently this traveling wave ends up in the far field. It was also shown that the radiation pattern for an electric multipole can be obtained from the result for a magnetic multipole, given by Eqs. (64) and (65), simply by an exchange of the Fresnel coefficients for s- and p-polarized waves.

The author's e-mail address is arnoldus @ra.msstate.edu.

REFERENCES

1. K. H. Drexhage, "Interaction of light with monomolecular dye layers," Prog. Opt. **12**, 163–232 (1974).
2. R. R. Chance, A. Prock, and R. Silbey, "Molecular fluorescence and energy transfer near interfaces," Adv. Chem. Phys. **39**, 1–65 (1978).
3. G. W. Ford and W. H. Weber, "Electromagnetic effects on a molecule at a metal surface," Surf. Sci. **109**, 451–481 (1981).
4. P. Goy, J. M. Raimond, M. Gross, and S. Haroche, "Observation of cavity-enhanced single-atom spontaneous emission," Phys. Rev. Lett. **50**, 1903–1906 (1983).
5. G. W. Ford and W. H. Weber, "Electromagnetic interactions of molecules with metal surfaces," Phys. Rep. **113**, 195–287 (1984).
6. R. G. Hulet, E. S. Hilfer, and D. Kleppner, "Inhibited spontaneous emission by a Rydberg atom," Phys. Rev. Lett. **55**, 2137–2140 (1985).
7. W. Jhe, A. Anderson, E. A. Hinds, D. Meschede, L. Moi, and S. Haroche, "Suppression of spontaneous decay at optical frequencies: test of vacuum-field anisotropy in confined space," Phys. Rev. Lett. **58**, 666–669 (1987).
8. D. J. Heinzen, J. J. Childs, J. E. Thomas, and M. S. Feld, "Enhanced and inhibited visible spontaneous emissions by atoms in a confocal resonator," Phys. Rev. Lett. **58**, 1320–1323 (1987).
9. G. S. Agarwal, "Coherence in spontaneous emission in the presence of a dielectric," Phys. Rev. Lett. **32**, 703–706 (1974).
10. W. Lukosz and R. E. Kunz, "Light emission by magnetic and electric dipoles close to a plane interface. I. Total radiated power," J. Opt. Soc. Am. **67**, 1607–1615 (1977).
11. W. Lukosz, "Theory of optical-environment-dependent spontaneous-emission rates for emitters in thin layers," Phys. Rev. B **22**, 3030–3038 (1980).
12. W. Lukosz and R. E. Kunz, "Light emission by magnetic and electric dipoles close to a plane interface. II. Radiation patterns of perpendicular oriented dipoles," J. Opt. Soc. Am. **67**, 1615–1619 (1977).
13. H. F. Arnoldus and J. T. Foley, "Transmission of dipole radiation through interfaces and the phenomenon of anticritical angles," J. Opt. Soc. Am. A **21**, 1109–1117 (2004).
14. B. Hecht, "Forbidden light scanning near-field optical microscopy," Ph.D. thesis (University of Basel, Basel, Switzerland, 1996).
15. L. Novotny, D. W. Pohl, and P. Regli, "Light propagation through nanometer-sized structures: the two-dimensional-aperture scanning near-field optical microscope," J. Opt. Soc. Am. A **11**, 1768–1779 (1994).
16. H. Heinzelmann, B. Hecht, L. Novotny, and D. W. Pohl, "Forbidden light scanning near-field optical microscopy," J. Microsc. **177**, 115–118 (1995).
17. D. Van Labeke, F. Baida, D. Barchiesi, and D. Courjon, "A theoretical model for the inverse scanning tunneling optical microscope (ISTOM)," Opt. Commun. **114**, 470–480 (1995).
18. G. A. Massey, "Microscopy and pattern generation with scanned evanescent waves," Appl. Opt. **23**, 658–660 (1984).
19. J. M. Vigoureux, F. Depasse, and C. Girard, "Superresolution of near-field optical microscopy defined from properties of confined electromagnetic waves," Appl. Opt. **31**, 3036–3045 (1992).
20. D. Van Labeke, D. Barchiesi, and F. Baida, "Optical characterization of nanosources used in scanning near-field optical microscopy," J. Opt. Soc. Am. A **12**, 695–703 (1995).
21. B. Hecht, D. W. Pohl, and H. Heinzelmann, "Tunnel near-field optical microscopy: TNOM-2," in *Photons and Local Probes*, O. Marti and R. Möller, eds. (Kluwer, Dordrecht, The Netherlands, 1995), pp. 93–107.
22. B. Hecht, H. Bielefeldt, and D. W. Pohl, "Influence of detection conditions on near-field optical imaging," J. Appl. Phys. **84**, 5873–5882 (1998).
23. H. F. Arnoldus and J. T. Foley, "Spatial separation of the traveling and evanescent parts of dipole radiation," Opt. Lett. **28**, 1299–1301 (2003).
24. M. E. Rose, *Multipole Fields* (Wiley, New York, 1955).
25. J. M. Eisenberg and W. Greiner, *Excitation Mechanisms of the Nucleus* (North-Holland, Amsterdam, The Netherlands, 1970), Chap. 3.
26. M. E. Rose, *Elementary Theory of Angular Momentum* (Dover, New York, 1995), Chap. 7.
27. J. D. Jackson, *Classical Electrodynamics*, 3rd ed. (Wiley, New York, 1999), p. 441.
28. A. J. Devaney and E. Wolf, "Multipole expansion and plane wave representations of the electromagnetic field," J. Math. Phys. **15**, 234–244 (1974).
29. H. F. Arnoldus, "Angular spectrum representation of the electromagnetic multipole fields," submitted to J. Math. Phys.
30. A. Erdélyi, "Zur Theory der Kugelwellen," Physica (Utrecht) **4**, 107–120 (1937).
31. J. E. Sipe, "The dipole antenna problem in surface physics: a new approach," Surf. Sci. **105**, 489–504 (1981).
32. J. E. Sipe, "New Green function formalism for surface optics," J. Opt. Soc. Am. B **4**, 481–489 (1987).
33. J. Gasper, G. C. Sherman, and J. J. Stamnes, "Reflection and refraction of an arbitrary electromagnetic wave at a plane interface," J. Opt. Soc. Am. **66**, 955–961 (1976).
34. G. C. Sherman, J. J. Stamnes, and E. Lalor, "Asymptotic approximations to angular-spectrum representations," J. Math. Phys. **17**, 760–776 (1976).
35. M. Born and E. Wolf, *Principles of Optics*, 7th (expanded) ed. (Cambridge U. Press, Cambridge, UK, 1999), App. III, p. 890.